

The Cilium- and Centrosome-Associated Protein CCDC11 Is Required for Cytokinesis via Midbody Recruitment of the ESCRT-III Membrane Scission Complex Subunit CHMP2A

Arooba Ahmed^{1*}, Jiachen Lee^{1*}, Jillian E. Parker^{2*}, Alia Rizvon¹, Vishal Nyayapathi¹, Feng-Qian Li³, Michael W. Lake^{1,2,4} and Ken-Ichi Takemaru^{3†}

¹Half Hollow Hills High School East, ²Half Hollow Hills High School West, Dix Hills, NY 11746

³Department of Pharmacological Sciences, Stony Brook University, Stony Brook, NY 11794

⁴Department of Biochemistry and Cell Biology, Stony Brook University, Stony Brook, NY 11794

*These authors contributed equally to this work and are listed in alphabetical order.

†Correspondence email: ken-ichi.takemaru@stonybrook.edu

Summary

Cell division is a fundamental biological process, crucial for the normal development of an organism as well as tissue repair, regeneration, and wound healing. During cell division, there are multiple critical checkpoints that ensure accurate replication and distribution of DNA. The final stage, cytokinesis, involves the physical separation of two newly formed daughter cells. Our research focused on elucidating the molecular functions of the coiled-coil domain-containing 11 (CCDC11) protein, which has been associated with human laterality disorders and plays critical roles in the formation and function of cilia, hair-like structures on the apical cell surface. We found that, in addition to cilia, CCDC11 localizes to the cleavage furrow and midbody between two dividing daughter cells of various human cell lines. CCDC11 contains three coiled-coil (CC) domains, and the CC1 and CC2 domains are responsible for its midbody localization. We also observed that depletion of CCDC11 results in a significant increase in the number of multinucleated cells, indicating defects in cytokinesis, the final stage of cell division. Furthermore, CCDC11-depleted cells exhibit diminished midbody recruitment of the protein CHMP2A, a critical component of the ESCRT-III membrane scission machinery. Collectively, our findings uncover a novel and previously unreported role for CCDC11 in cytokinesis.

Received: December 7, 2017; **Accepted:** February 5, 2018; **Published:** March 14, 2018

Copyright: (C) 2018 Ahmed *et al.* All JEI articles are distributed under the attribution non-commercial, no derivative license (<http://creativecommons.org/licenses/by-nc-nd/3.0/>). This means that anyone is free to share, copy and distribute an unaltered article for non-commercial purposes provided the original author and source is credited.

Introduction

The coiled-coil domain-containing 11 (CCDC11) protein is a 62-kDa polypeptide that is associated with

both ciliary and centriolar satellite structures (1-3). Cilia are microtubule-based hair-like organelles that protrude from the apical cell surface and perform a wide range of biological tasks including environmental sensing, cellular signaling, and establishment of left-right asymmetry (4-6). Previous proteomic studies have identified over 1,200 ciliary proteins in humans (7). However, how these proteins function during ciliogenesis or other biological processes is not well understood. Dysfunctional cilia have been linked to a variety of human disorders including polycystic kidney disease, blindness, mental disorders, and obesity, collectively known as ciliopathies (4-6). While the function of motile nodal cilia in the establishment of left-right asymmetry has been well-documented (8), the role of CCDC11 in this process has only recently been elucidated through the identification of four unique human CCDC11 mutations that result in various laterality disorders including dextrocardia, heterotaxia, and situs inversus (2, 9). However, the precise molecular function of CCDC11 remains poorly understood, and whether CCDC11 plays a role beyond ciliogenesis is currently unknown.

Here we report that CCDC11 plays a critical role in cytokinesis in human cell lines by promoting the recruitment of CHMP2A, which is a component of the endosomal sorting complex required for transport III (ESCRT-III). Cytokinesis is the final phase of cell division by which a single cell physically separates into two daughter cells (10, 11). At the end of cytokinesis, ESCRT-III splits the intercellular membrane bridge between nascent daughter cells in a process known as abscission (11-13). Although four ESCRT complexes have been characterized (ESCRTs-0, -I, -II, and -III), ESCRTs-I and -III appear to be predominantly required for cytokinesis (11-13). Besides cytokinetic abscission, ESCRTs have also been implicated in a wide array of cellular processes requiring an internal membrane fission event including viral budding, plasma and nuclear

membrane repair, and neuronal pruning (14, 15).

Towards the completion of cytokinesis, ESCRT-I promotes the recruitment of the membrane scission machinery, ESCRT-III, to the midbody, which is a transient structure in the center of the intercellular bridge between two daughter cells (10, 11). Assembly of ESCRTs-I and -III, as well as accessory proteins, at the midbody and subsequent abscission are temporally regulated in part by the mitotic kinases polo-like kinase 1 (Plk1) and cyclin-dependent kinase 1 (Cdk1) (10, 11, 16). Once anaphase is initiated, the activity of both Plk1 and Cdk1 declines, triggering the binding of protein regulator of cytokinesis 1 (PRC1) to antiparallel microtubules of the central spindle apparatus (16, 17). Subsequently, the 55 kDa centrosomal protein (CEP55) is recruited to the central spindle and midbody (18, 19). CEP55 is critical for abscission as it facilitates the recruitment of both ESCRT-I and ESCRT-III via its direct interactions with the ESCRT-I subunit tumor-susceptibility gene 101 (Tsg101) and the adapter protein apoptosis-linked gene-2 interacting protein X (Alix), respectively (11, 12, 14). Recruitment of Tsg101/ESCRT-I and Alix to the midbody provides a targeting platform for the ESCRT-III complex subunits, collectively referred to as charged multivesicular body proteins (CHMPs). Humans express eleven distinct ESCRT-III proteins that can be sorted into seven different classes (CHMP1-7) (11, 12). CHMPs assemble into functional membrane-associated ESCRT-III filaments, which in conjunction with the AAA-ATPase Vps4, form circular/spiral arrays that deform membranes, inducing alterations in curvature, resulting in membrane scission (11, 12). Interestingly, ESCRT proteins are present in cilia (20), but their precise roles in ciliogenesis remain to be elucidated.

In an effort to study the subcellular distribution of CCDC11 in detail, we found that CCDC11 localized

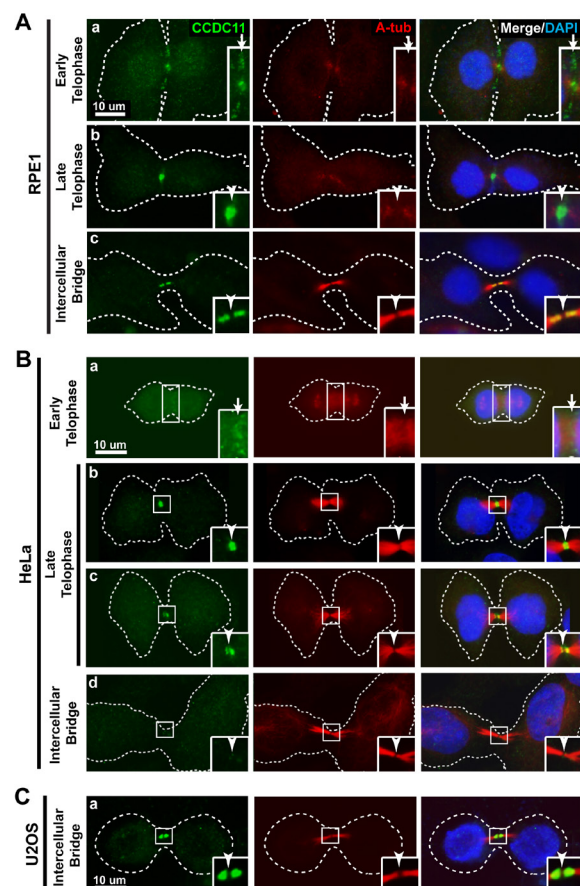
to the midbody region in multiple human cell types, as well as the centrosomal and ciliary structures. We then hypothesized that it functions in cytokinesis. To test our hypothesis, we eliminated endogenous CCDC11 protein from cells by small interfering RNA (siRNA) and examined the effects of CCDC11 loss on cell division and recruitment of cytokinesis proteins. Depletion of CCDC11 led to an increase in the number of multinucleated cells, suggesting defects in cytokinesis. We also found that CCDC11 promotes the efficient recruitment of the ESCRT-III component CHMP2A. This suggests that CCDC11 plays a crucial role in cytokinesis beyond its known ciliary roles.

Results

Endogenous CCDC11 dynamically localizes to the cleavage furrow and midbody region in cells

To investigate the subcellular localization of endogenous CCDC11, we chose three different human cell lines, retinal pigment epithelial (RPE1) cells, cervical cancer HeLa cells, and osteosarcoma U2OS cells, as they are widely used experimental model systems in cell biology. These cells were co-immunostained with antibodies against CCDC11 and acetylated α -tubulin

Figure 1. Endogenous CCDC11 localizes to the midbody region during cytokinesis in RPE1, HeLa, and U2OS cells. RPE1, HeLa and U2OS cells were co-immunostained with antibodies for CCDC11 (green) and acetylated α -tubulin (A-tub, red) to visualize endogenous proteins. Nuclei were stained using DAPI (blue). (A) In RPE1 cells, during early telophase (a), CCDC11 became enriched at the cleavage furrow (arrows). In late telophase and intercellular bridge, CCDC11 was observed at the midbody (A-tub-negative dark zones, arrowheads) and flanking regions, respectively. (B) Similar localization patterns were detectable in HeLa cells except that CCDC11 levels were severely reduced or lost in the midbody region in the intercellular bridge (d). (C) In contrast to RPE1 and HeLa cells, CCDC11 signals were only detectable in the intercellular bridge in U2OS cells as it localized to two cortical regions adjacent to the midbody (arrowheads). Dashed lines represent cell boundaries. The insets show zoomed images of the squared areas.



(A-tub). A-tub is a hallmark of stabilized microtubules, and microtubules in cilia are highly acetylated. In RPE1 cells (**Figure 1A**), during early stages of telophase, the final stage of mitosis, CCDC11 was clearly detectable at the cleavage furrow (**Figure 1Aa**). During late telophase, CCDC11 became intensely enriched at the midbody, which was indicated by the dark gap between the A-tub-positive structures (**Figure 1Ab**). In the intercellular bridge, as cytokinesis proceeded, CCDC11 localized to the broad regions adjacent to the midbody (**Figure 1Ac**).

In HeLa cells, during early telophase, there was faint yet consistent CCDC11 staining at the cleavage furrow (**Figure 1Ba**). During late telophase, prominent CCDC11 fluorescence was observed at the midbody (**Figure 1Bb**) or at the flanking regions of the midbody (**Figure 1Bc**). Later in the intercellular bridge, CCDC11 signals were weak or completely lost (**Figure 1Bd**), suggesting that it dissociates from the midbody prior to the completion of cytokinesis.

Next, we performed immunofluorescence staining for CCDC11 and A-tub in U2OS cells grown to sub-confluence. The endogenous CCDC11 was detectable at the flanking zones of the midbody (**Figure 1Ca**). Unlike in RPE1 and HeLa cells, CCDC11 was only observable at the midbody flanking region in the intercellular bridge in U2OS cells, while undetectable earlier in telophase. This suggests that the midbody localization of CCDC11 might be regulated in a cell-type specific manner. Collectively, our data demonstrate that CCDC11 localizes to the midbody region in three different cell lines and suggest a novel conserved role for CCDC11 in the successful completion of cytokinesis across multiple different cell types.

Endogenous CCDC11 localizes to centrioles in HeLa and U2OS cells

CCDC11 has been shown to localize to centrioles and centriolar satellites, and its function is essential for the formation and function of cilia in RPE1 cells, zebrafish, and *Xenopus* embryos (1-3). However, whether CCDC11 similarly shows centriolar localization in cell types that do not form cilia had not been examined. HeLa and U2OS cells rarely form cilia. Thus, we determined the centriolar localization of endogenous CCDC11 using immunofluorescence staining for CCDC11 and A-tub in HeLa and U2OS cells at sub-confluence. CCDC11 was detected at A-tub-positive centrioles in both HeLa (**Figure 2a**) and U2OS (**Figure 2b**) cells. This suggests that CCDC11 is present at centrioles in cell types that do not typically possess cilia and raises the possibility that, besides cilogenesis, CCDC11 may play an additional, unknown role at centrioles in non-ciliated cell types.

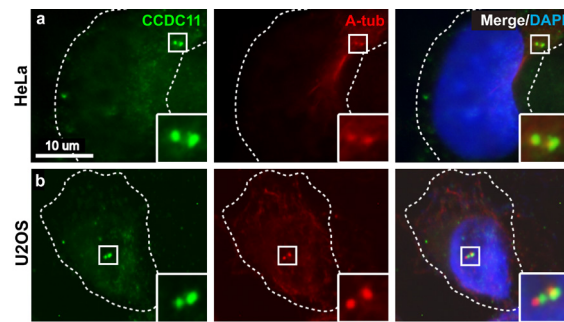


Figure 2. Endogenous CCDC11 localizes to centrioles in HeLa and U2OS cells. HeLa (a) and U2OS (b) cells were co-labelled with antibodies for CCDC11 (green) and A-tub (red). Nuclei were stained using DAPI (blue). Dashed lines represent cell boundaries, and two centrioles are enlarged in the insets. CCDC11 localized to both mother and daughter centrioles in U2OS and HeLa cells.

Ectopically expressed CCDC11 localizes to the midbody in U2OS cells

In addition to the localization of endogenous CCDC11, we also analyzed the subcellular distribution of ectopically expressed CCDC11. U2OS cells were employed for subsequent experiments because of their high transfection efficiency. U2OS cells were transiently transfected with an expression plasmid for myc-tagged full-length CCDC11 (CCDC11-FL) for 48 hours before being fixed on coverslips for staining. Immunofluorescence staining for the myc tag and A-tub revealed that ectopic CCDC11-FL, like the endogenous protein, was detectable at the midbody (**Figure 3Aa**). However, it was noted that ectopic CCDC11-FL localized to the midbody instead of the regions adjacent to the midbody to which endogenous CCDC11 localized (**Figure 1Ca**). Ectopic CCDC11-FL also showed centriolar localization (**Figure 3Ae**).

Next, we used various CCDC11 deletion mutants to determine the roles of the three different coiled-coil (CC) domains in its midbody localization (**Figure 3B**). CCDC11-patient mutation (PM) (1-332+17) is derived from human patients with abnormal left-right asymmetry (21). The mutation causes a deletion of CC3, which results from a frameshift that leads to the incorporation of 17 extra amino acids as well as a premature stop codon. As shown in **Figure 3Ab**, CCDC11-PM exhibited a clear midbody localization. In marked contrast, the midbody signal of CCDC11 (1-175) containing only CC1 (**Figure 3Ac**) and CCDC11 (176-514) containing CC2 and CC3 (**Figure 3Ad**) was undetectable or dramatically reduced in comparison to CCDC11-FL. These results indicate that both CC1 and CC2 are required for the efficient midbody localization of CCDC11. It is worth noting that CC1 and CC2 are also responsible for the centriolar

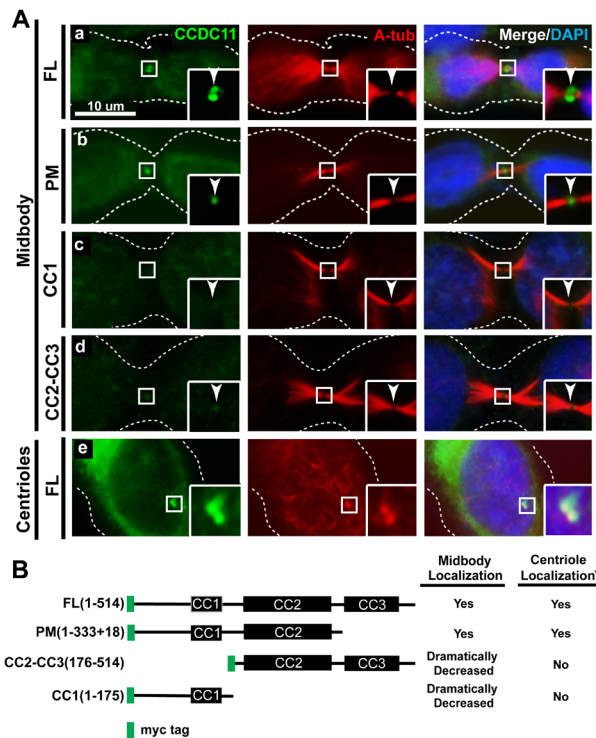


Figure 3. Ectopically expressed CCDC11 localizes to the midbody region in U2OS cells. (A) U2OS cells were transiently transfected with expression plasmids for myc-tagged CCDC11 full-length (FL), patient mutation (PM), CC2-CC3, or CC1 as illustrated in (B) and co-stained using anti-myc antibody (green) and anti-A-tub (red) antibody. Nuclei were detected using DAPI (blue). Both FL (a) and PM (b) localized to the midbody, whereas the midbody localization of CC2-CC3 (c) and CC1 (d) was dramatically reduced. (e) Clear centriolar localization was observed for FL but not for PM (data not shown). (B) Schematic diagram of different CCDC11 deletion mutants used in this study and summary of the results from (A). Green boxes indicate myc tag at the N-terminus. *Centriolar localization results adapted from Silva *et al.*, 2015 (1).

targeting of CCDC11 (Figure 3B) (1), suggesting that CCDC11 traffics to the centrioles and midbody through a similar mechanism.

CCDC11 knockdown causes significant decrease at the midbody in U2OS cells

We used small interfering RNA-mediated knockdown (siRNA-KD) to examine the potential effects of CCDC11 depletion on cytokinesis. The previously validated siRNA targeting the coding region of the human CCDC11 gene was utilized to knockdown endogenous CCDC11 in U2OS cells (1). U2OS cells treated with CCDC11 siRNA showed significantly reduced levels of CCDC11 at the midbody region compared to those transfected with a randomized control siRNA (Figure 4). Therefore, we

concluded that CCDC11 siRNA successfully decreased CCDC11 protein levels at the midbody in U2OS cells and could be used to evaluate the effect of CCDC11 KD on cytokinesis.

Endogenous CCDC11 knockdown leads to increased instances of multinucleated cells

Cytokinesis failure often results in multinucleation (22, 23). To determine whether CCDC11 plays a role in cytokinesis, U2OS cells were transfected with either CCDC11 or control siRNA for 48 hours, fixed, and immunostained for A-tub and β -catenin, which marks cell boundaries, and nuclei were stained with DAPI. The numbers of bi- and multinucleated cells were counted. CCDC11 KD yielded an increase in the numbers of bi- and multinucleated cells (Figure 5A). Quantification analyses revealed that CCDC11 KD increased the number of binucleated cells 3.5-fold as compared to control cells (control siRNA, 4.8% \pm 0.6%; CCDC11 siRNA, 16.7% \pm 2.9%; $p < 0.05$) (Figure 5B). CCDC11 KD also increased the number of multinucleated cells 2.9-fold as compared to control cells (control siRNA, 0.9% \pm 0.26%; CCDC11 siRNA, 2.6% \pm 0.21%; $p < 0.01$). These results indicate that CCDC11 KD interferes with the completion of cytokinesis, leading to multinucleation. Since CCDC11 localizes to the midbody region (Figure 1), this suggests that CCDC11 is involved in cytokinesis. However, binucleation may be caused by other mechanisms such as multipolar spindles and fusion of two cells (24). Live-cell imaging experiments may distinguish between these possibilities. We expect that CCDC11 KD would similarly lead to increased incidence of multinucleation in RPE1 and HeLa cells, since CCDC11 also localizes to the midbody.

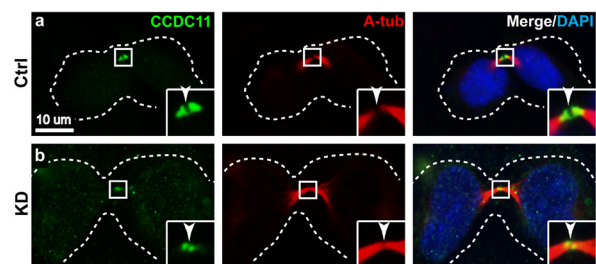


Figure 4. Diminished CCDC11 protein levels at the midbody upon siRNA-mediated KD in U2OS cells. U2OS cells were treated with either control (Ctrl) or CCDC11 (KD) siRNA and then immunostained for CCDC11 (green) and A-tub (red) 48 hours post-transfection. Nuclei were stained with DAPI (blue).

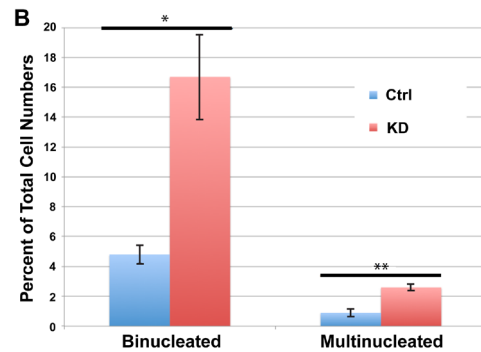
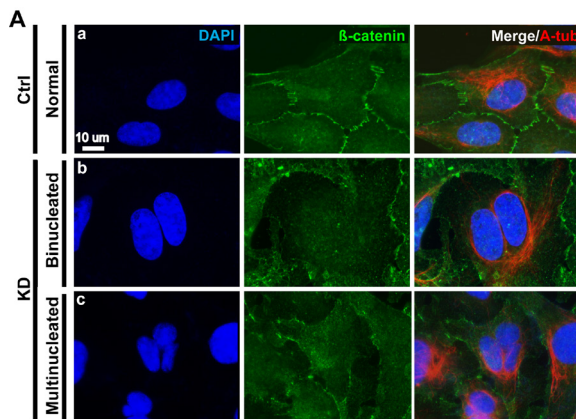


Figure 5. CCDC11 KD causes multinucleation in U2OS cells. (A) U2OS cells were transfected with either control (Ctrl) or CCDC11 (KD) siRNA, fixed 48 hours after transfection, and stained for the cell boundary marker β -catenin (green) and A-tub (red). The nuclei were stained using DAPI (blue). Representative images of normal control (a), binucleated (b), and multinucleated (c) CCDC11-KD cells are shown. (B) Quantification of multinucleated cells. Percentages were calculated as (numbers of binucleated or multinucleated cells/total numbers of cells) \times 100. The CCDC11-KD cells showed increased instances of both binucleation and multinucleation. A total of 768 and 627 cells were counted for control and CCDC11-KD cells, respectively, from three independent experiments. * $p < 0.05$; ** $p < 0.01$.

CCDC11 recruits the ESCRT-III component CHMP2A to the midbody

We then examined possible changes in the localization of the known midbody proteins PRC1, CEP55, and CHMP2A in CCDC11-KD U2OS cells to gain insight into the molecular mechanisms underlying their cytokinesis defects. U2OS cells were transfected with either control or CCDC11 siRNA and immunostained for A-tub and PRC1, CEP55, or CHMP2A (Figure 6A). PRC1 and CEP55 showed no obvious changes in their midbody localization in CCDC11-KD cells (Figure 6Ab and 6Ad) in comparison to control cells (Figure 6Aa and 6Ac). However, there was a dramatic reduction in CHMP2A fluorescence at the flanking regions of the midbody in CCDC11-KD cells (Figure 6Af) compared to control cells (Figure 6Ae). Quantification analyses of the number of cells with reduced CHMP2A fluorescence at the midbody region revealed that 90% of CCDC11-KD cells exhibited a dramatic reduction in CHMP2A midbody localization, whereas 85% of control cells showed bright CHMP2A fluorescence at the midbody region (Figure 6B). Taken together, these findings suggest that CCDC11 promotes the recruitment of CHMP2A and likely the ESCRT-III machinery to the midbody to facilitate membrane scission at the final stage of cytokinesis.

Discussion

CCDC11 has been shown to be mutated in human laterality disorders and extensively studied in the context of ciliogenesis (1-3, 9, 21). However, its nonciliary roles remain largely unknown. In the work presented here, we demonstrated that CCDC11 localizes to the cleavage

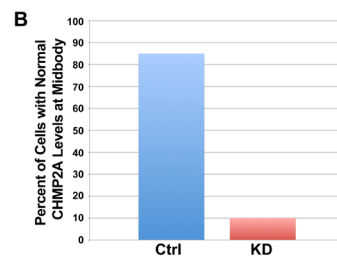
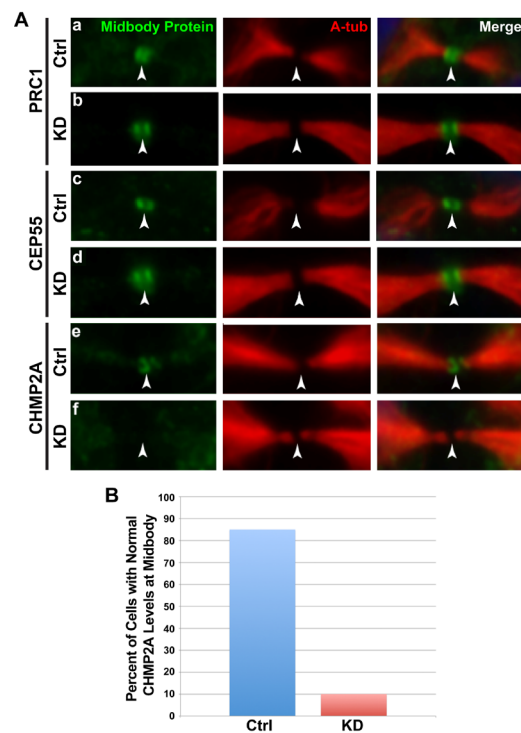


Figure 6. CCDC11 is required for proper recruitment of the ESCRT-III subunit CHMP2A to the midbody. (A) U2OS cells were treated with control (Ctrl) or CCDC11 (KD) siRNA, fixed 48 hours post-transfection, and co-stained for A-tub and different midbody markers as indicated. CCDC11 KD showed no significant effects on the midbody localization of PRC1 (a-b) and CEP55 (c-d) but led to a profound decrease in CHMP2A levels (e-f). (B) Quantification of U2OS cells with normal levels of CHMP2A at the midbody. A total of 20 cells undergoing abscission were counted for each of control and CCDC11-KD samples.

furrow and the midbody region and acts in cytokinesis by promoting midbody localization of the ESCRT-III subunit CHMP2A. Our results suggest a novel role for CCDC11 in promoting the efficient recruitment of ESCRT-III to the midbody during cytokinesis, likely allowing for the timely cleavage of the intercellular bridge (**Figure 7**).

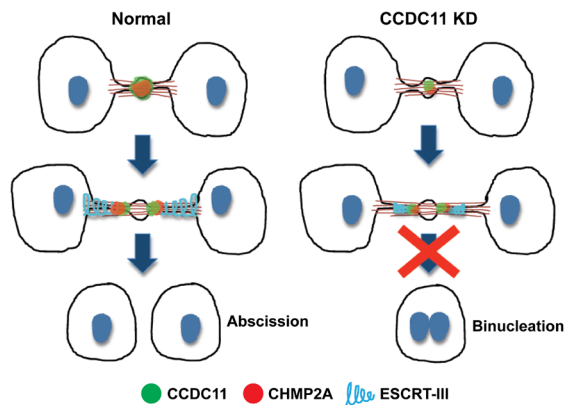


Figure 7. Model for the role of CCDC11 in cytokinesis. CCDC11 (green circles) facilitates the recruitment of CHMP2A (red circles) and likely other ESCRT-III components to the midbody. This may trigger the formation of ESCRT-III filaments (light blue coils), resulting in efficient abscission and production of two new daughter cells. CCDC11-KD cells fail to efficiently recruit CHMP2A, leading to insufficient assembly of the ESCRT-III machinery adjacent to the midbody, failure to complete membrane scission, and the appearance of binucleated cells.

Our experimental results support emerging evidence of pleiotropic protein function and considerable overlap between the molecular processes of ciliogenesis and cytokinesis. It has been reported that the midbody proteins PRC1 and MKLP-1 localize to the basal bodies of ciliated epithelial cells (25), and that Vps4, Alix, and other ESCRT components are present at ciliary transition zones (20). Intriguingly, CCDC11 targeting to the midbody depends on the same CC1 and CC2 domains responsible for its recruitment to centrosomes (1). These findings raise the possibility that aberrant laterality phenotypes in patients with CCDC11 mutations may, in part, also result from inefficient cytokinesis and/or these patients may manifest additional phenotypes associated with cytokinesis defects. Of note, in our study, a CC2-only deletion was not tested, and hence we cannot formally exclude the possibility that the combined deletion of CC2 and CC3 has a different effect than either individual deletion at present. Our study also highlights a potential global cellular role for CCDC11 in ESCRT-III recruitment and scission wherever an internal membrane fission event is required. It would be of great interest to investigate if CCDC11 is found at the sites of

viral budding, neural pruning, autophagosome closure, and multivesicular endosomes where ESCRT-III is known to function (14, 15).

Although not entirely consistent between the human cell lines examined (**Figure 1**), CCDC11 appeared to be slightly enriched at the cleavage furrow in early telophase, to concentrate at the midbody during late telophase, and finally to localize to the positions adjacent to the midbody in the intercellular bridge during late cytokinesis and abscission. Worthy of note, this localization pattern is similar to that of CHMP2A during cytokinesis (13). This suggests that CCDC11 may recruit CHMP2A to the midbody either directly, possibly through mutual coiled-coil domains found in both proteins, or indirectly via interactions with other ESCRT-III proteins to promote ESCRT-III oligomerization and filament formation. CCDC11-KD cells failed to recruit sufficient CHMP2A (**Figure 6**), most likely leading to minimal or complete absence of ESCRT-III filaments.

Based on our findings that both the CC1 and CC2 domains of CCDC11 are involved in its localization to the midbody, along with the abundance of coiled-coil domain-containing proteins present at the midbody (PRC1, MKLP-1, CYK-4, Cep55, Alix, Tsg101, and Centriolin) (10-13), it is reasonable to hypothesize that CCDC11 interacts with one or multiple coiled-coil domain-containing proteins to execute its function. Similarly, CCDC11 could serve as an adapter protein, binding to any CHMPs through their N-terminal coiled-coil domains. In addition, many of the CHMP/ESCRT-III interactions with AAA-ATPase Vps4 and other accessory proteins are known to be mediated through MIT (microtubule interacting and trafficking)-MIM (MIT-interacting motif) amphipathic helical structures. Upon inspection of the CCDC11 protein sequence, we found two MIM-like sequences in its CC2 domain (26). Both CCDC11 MIM-like sequences reveal an amphipathic nature, possessing a hydrophobic face opposite a highly charged helical surface. Thus, like the CHMP2A MIM sequence, these putative CCDC11 MIM sequences may be involved in additional protein-protein interactions with midbody proteins harboring MIT domains.

To further elucidate the role of CCDC11 in cytokinesis, it would be interesting to determine the functional importance of its CC domains individually or in combination in cytokinesis. In addition, it would be valuable to examine protein-protein interactions with other components of ESCRT-III, such as CHMP1, CHMP3, CHMP4, and CHMP6, as well as proteins involved in abscission, including Vps4. This would allow the roles of CCDC11 to be examined thoroughly, shedding light on whether a direct or indirect interaction exists with the ESCRT-III complex. Live-cell imaging analysis might be helpful in order to observe cytokinesis

in real-time to better understand the defects associated with CCDC11 mutations. We used *in vitro* tissue culture cell models in this study, so it would be important to examine human patients and animal models for possible cytokinesis defects in an *in vivo* setting. Since ESCRT-III is crucial for a variety of biological processes including neural pruning and viral budding in addition to cytokinesis (14, 15), it is possible that CCDC11 may play a critical role in these processes as well. Thus, our study has implications for a broad range of devastating diseases including cancer, neurodegenerative diseases, and viral infections.

Methods

Bacterial transformation and plasmid purification

Myc-tagged CCDC11 plasmids were transformed into *E. coli* DH5 α competent cells (New England BioLabs). Approximately 100 ng of each plasmid DNA was added to the competent cells, gently mixed, and placed on ice for 10 minutes. The competent cells were heat-shocked at 42°C for 45 seconds. Next, 1 mL of LB media without antibiotics was added to the tube, followed by incubation at 37°C for 45 minutes and centrifugation at 2,000 rpm for 2 minutes. The bacteria were plated onto a 10-cm agar plate containing 50 μ g/ml kanamycin (Sigma-Aldrich). Sterile glass beads were used to spread the cells evenly throughout the agar plate, and the plate was incubated overnight at 37°C. The next day, bacterial colonies were scraped, transferred into a 1 L flask containing 200 ml of LB media with 50 μ g/mL kanamycin, and grown overnight at 37°C in a shaker. Plasmid DNA was then purified using the Qiagen Midiprep Kit according to the manufacturer's instructions.

Tissue culture, transient transfection, and siRNA transfection

RPE1, HeLa, and U2OS cells were purchased from American Type Culture Collection (ATCC) and grown in Dulbecco's modified Eagle's medium (DMEM) with 10% fetal bovine serum (FBS) (Invitrogen) and 100 U/mL penicillin-streptomycin. Cells were seeded onto a 12-well plate, cultured overnight to 60-80% confluence, and transfected with CCDC11 plasmids using polyethylenimine (Sigma-Aldrich). For CCDC11-KD experiments in U2OS cells, the previously validated siRNA with 3'-TT overhangs (5'-GAGACGAACAGGACUUGAATT -3', 4392420, ID s47871) (1) and a negative control siRNA (Silencer Select Negative Control No.1, 4390844) were purchased from Ambion, Thermo Fisher Scientific. The siRNA was transfected using the RNAiMAX transfection reagent (Thermo Fisher Scientific) with Opti-MEM media (Thermo Fisher Scientific). Cells were transfected at 30-50% confluency and grown for 48 hours in a 37°C

incubator with 5% CO₂.

Immunofluorescence staining and microscopy

Glass coverslips were placed into the wells of 12-well plates in a tissue culture hood and exposed to a UV germicidal lamp for 15 minutes. RPE1, HeLa, and U2OS cells were seeded onto the wells and cultured overnight. Non-transfected or transfected cells were washed with PBS (phosphate-buffered saline) and fixed with cold 50% methanol/50% acetone. After washing with PBS, 300 μ l of blocking solution containing 5% goat serum in diluent solution (5% bovine serum albumin [BSA] and 0.2% Triton X-100 in PBS) was added to the cells, followed by incubation at room temperature for one hour. The blocking solution was removed, and the cells were incubated for one hour at room temperature in 300 μ l of diluent solution containing primary antibodies. The primary antibodies utilized were: rabbit anti-CCDC11 (Sigma-Aldrich, HPA040595, 1:300), mouse anti-acetylated α -tubulin (Sigma-Aldrich, T7451, 1:300), rabbit anti- β -catenin (Sigma-Aldrich, C2206, 1:300), mouse anti-myc (in house, 1:50), rabbit anti-CHMP2A (Proteintech, 10477-1-1AP, 1:300), rabbit anti-CEP55 (Proteintech, 23891-1-AP, 1:300), and rabbit anti-PRC1 (Abcam, ab21473, 1:300). The cells were then incubated for one hour in the dark with appropriate anti-rabbit or anti-mouse IgG secondary antibodies conjugated with DyLight 488 and DyLight 549 (Vector Laboratories), or anti-mouse IgG1 Alexa Fluor 488-conjugated antibody and anti-mouse IgG2b Alexa Fluor 555-conjugated antibody (Thermo Fisher Scientific). Cells were washed with PBS and counterstained with DAPI for two minutes at room temperature. The cells were then mounted onto a microscope glass slide with Fluoromount-G (SouthernBiotech) and sealed with nail polish. The slide was kept in the dark for 30 minutes to dry at room temperature and stored at 4°C.

Immunostained cells were viewed under a Leica DMI6000B epifluorescence microscope with a Leica DFC300 FX digital camera and Application Suite software. HCX PL Fluotar 100x/1.3NA and 63x/1.25NA oil objectives were used.

Quantification of multinucleated cells and CHMP2A recruitment

For quantification of multinucleated cells, 10 images were randomly taken for each immunostained slide containing U2OS cells treated with control or CCDC11 siRNA under the Leica DMI6000B microscope at 63x. Cells were then individually counted on computer screens for binucleation and multinucleation, and the percentages of total cell numbers were calculated. This process was repeated for two more independent experiments to create three trials. After data were

collected, Student's two-tailed t-tests were performed in Microsoft Excel, and a p -value <0.05 was considered statistically significant. For quantification of the midbody recruitment of CHMP2A, control and CCDC11-KD U2OS cells were immunostained for CHMP2A and A-tub, and cells undergoing cytokinesis were counted under the Leica DMI6000B microscope at 63x.

References

- Silva E, *et al.* "CCDC11 is a novel centriolar satellite protein essential for ciliogenesis and establishment of left-right asymmetry". *Mol Biol Cell* 27.1 (2016):48-63.
- Narasimhan V, *et al.* "Mutations in CCDC11, which encodes a coiled-coil containing ciliary protein, causes situs inversus due to dysmotility of monocilia in the left-right organizer". *Hum Mutat* 36.3 (2015): 307-18.
- Gur M, *et al.* "Roles of the cilium-associated gene CCDC11 in left-right patterning and in laterality disorders in humans". *Int J Dev Biol* 61.3.4.5 (2017): 267-76.
- Goetz SC, Anderson KV. "The primary cilium: a signalling centre during vertebrate development". *Nat Rev Genet* 11.5 (2015):331-44.
- Nigg EA & Raff JW. "Centrioles, centrosomes, and cilia in health and disease". *Cell* 139.4 (2009): 663-78.
- Hildebrandt F, Benzing T, Katsanis N. "Ciliopathies". *N Engl J Med* 364.16 (2011): 1533-43.
- Gherman A, Davis EE, Katsanis N. "The ciliary proteome database: an integrated community resource for the genetic and functional dissection of cilia". *Nat Genet* 38.9 (2006): 961-2.
- Shinohara K & Hamada H. "Cilia in Left-Right Symmetry Breaking". *Cold Spring Harb Perspect Biol* 9.10 (2017).
- Perles Z, *et al.* "A human laterality disorder associated with recessive CCDC11 mutation". *J Med Genet* 49.6 (2012): 386-90.
- Eggert US, Mitchison TJ, Field CM. "Animal cytokinesis: from parts list to mechanisms". *Annu Rev Biochem* 75 (2006): 543-66.
- Mierzwa B & Gerlich DW. "Cytokinetic abscission: molecular mechanisms and temporal control". *Dev Cell* 31.5 (2014): 525-38.
- Nahse V, Christ L, Stenmark H, Campsteijn C. "The Abscission Checkpoint: Making It to the Final Cut". *Trends Cell Biol* 27.1 (2017): 1-11.
- Olmos Y Carlton JG. "The ESCRT machinery: new roles at new holes". *Curr Opin Cell Biol* 38 (2016):1-11.
- Christ L, Raiborg C, Wenzel EM, Campsteijn C, Stenmark H. "Cellular Functions and Molecular Mechanisms of the ESCRT Membrane-Scission Machinery". *Trends Biochem Sci* 42.1 (2017): 42-56.
- Alfred V & Vaccari T. "When membranes need an ESCRT: endosomal sorting and membrane remodelling in health and disease". *Swiss Med Wkly* 146 (2016): w14347.
- Bruinsma W, Raaijmakers JA, Medema RH. "Switching Polo-like kinase-1 on and off in time and space". *Trends Biochem Sci* 37.12 (2012):534-42.
- Hu CK, Ozlu N, Coughlin M, Steen JJ, Mitchison TJ. "Plk1 negatively regulates PRC1 to prevent premature midzone formation before cytokinesis". *Mol Biol Cell* 23.14 (2012): 2702-11.
- Zhao WM, Seki A, Fang G. "Cep55, a microtubule-bundling protein, associates with centralspindlin to control the midbody integrity and cell abscission during cytokinesis". *Mol Biol Cell* 17.9 (2009): 3881-96.
- Bastos RN & Barr FA. "Plk1 negatively regulates Cep55 recruitment to the midbody to ensure orderly abscission". *J Cell Biol* 191.4 (2010): 751-60.
- Diener DR, Lupetti P, & Rosenbaum JL. "Proteomic analysis of isolated ciliary transition zones reveals the presence of ESCRT proteins". *Curr Biol* 25.3 (2015): 379-84.
- Noel ES, *et al.* "A Zebrafish Loss-of-Function Model for Human CFAP53 Mutations Reveals Its Specific Role in Laterality Organ Function". *Hum Mutat* 37.2 (2016):194-200.
- van de Ven RA, *et al.* "p120-catenin prevents multinucleation through control of MKLP1- dependent RhoA activity during cytokinesis". *Nat Commun* (2016) 7:13874.
- Low SH, *et al.* "Syntaxin 2 and endobrevin are required for the terminal step of cytokinesis in mammalian cells". *Dev Cell* 4.5 (2003): 753-9.
- Shi Q & King RW. "Chromosome nondisjunction yields tetraploid rather than aneuploid cells in human cell lines". *Nature* 437.7061 (2005): 1038-42.
- Smith KR, *et al.* "A role for central spindle proteins in cilia structure and function". *Cytoskeleton (Hoboken)* 68.2 (2011):112-24.
- Guo EZ, Xu Z. "Distinct mechanisms of recognizing endosomal sorting complex required for transport III (ESCRT-III) protein IST1 by different microtubule interacting and trafficking (MIT) domains". *J Biol Chem* 290.13 (2015): 8396-408.

Acknowledgments

We would like to thank Drs. Moe Mahjoub and Ewelina Betleja at Washington University for the CCDC11 expression constructs. This work was supported in part by funds from NIH/NHLBI to K.I. Takemaru (R01HL107493 and R56HL107493). Publication of this work was supported by Addgene, a non-profit repository for life science resources.